Reduction Process in CeO_2−MO and CeO_2−M_2O_3 Mixed Oxides: A Computer Simulation Study

Gabriele Balducci,*,† M. Saiful Islam,‡ Jan Kašpar,† Paolo Fornasiero,† and Mauro Graziani†

Dipartimento di Scienze Chimiche, Universita' degli Studi di Trieste, via L.Giorgieri, 1, 34127 Trieste, Italy, and Department of Chemistry, University of Surrey, Guildford, Surrey, GU2 7XH, U.K.

Received August 14, 2002. Revised Manuscript Received March 10, 2003

A computer simulation study of the Ce^{4+}/Ce^{3+} reduction process in CeO_2−MO (M = Ca, Mn, Ni, Zn) and CeO_2−M_2O_3 (M = Sc, Mn, Y, Gd, La) mixed oxides is presented. Calculations satisfactorily reproduce the observed structural parameters of the solid solutions over a wide range of compositions. On energetic grounds, the Ce^{4+}/Ce^{3+} reduction process is enhanced with increasing dopant content, with the enhancement being more pronounced for divalent dopants. For a fixed dopant level, the reduction of cerium is more favorable for larger dopant ions. The results are explained in terms of the higher oxygen vacancy concentration and the larger dopant size being effective in accommodating the greater relaxation or elastic strain associated with forming the larger Ce^{3+} species upon reduction.

Introduction

The ability of ceria (CeO_2) to reversibly exchange oxygen is a key feature in its applications. The process can be represented with the following equation:

$$CeO_2 \rightleftharpoons CeO_{(2-x)} + \frac{1}{2}\, x\, O_{2(g)} \qquad (1)$$

which shows that this material can behave as an oxygen buffer, absorbing or releasing oxygen in response to the oxygen partial pressure of the surroundings. This is one of the reasons ceria-based mixed oxides are currently receiving great attention in the field of catalytic converters for the treatment of vehicle exhaust gases. For optimum catalytic activity, the air-to-fuel ratio in the exhaust mixture must be as close as possible to the stoichiometric value.[1]

Reaction 1 is sensitive to the presence of dopants in the fluorite-type structure of ceria. For instance, a great deal of experimental evidence indicates that the Ce^{4+}/Ce^{3+} reduction is greatly enhanced when zirconia (ZrO_2) is mixed with ceria to form a solid solution.[2−4] Temperature-programmed reduction (TPR) experiments also indicate a large bulk participation in the reduction process.[5] In previous studies[6−9] we have used computational techniques to elucidate the fundamental aspects of this promotion in $Ce_{1-x}M_xO_2$ solid solutions, where M represents the isovalent cations Zr^{4+}, Th^{4+}, and Hf^{4+}. Our reduction energies are consistent with the observation that the catalytic activity is enhanced by the introduction of Zr into CeO_2, which is associated with increased reducibility of the bulk mixed oxide.

Active research is presently devoted to improving the oxygen buffering ability of ceria. One of the followed strategies consists of doping ceria with tri- or divalent cations:[10−13] the consequent creation of oxygen vacancies in the material[14] is thought to favor its reducibility.[15,16] In addition to catalytic applications, acceptor-doped ceria (especially Gd-doped ceria) has attracted considerable interest for use in electrochemical devices such as solid oxide fuel cells (SOFCs).[17−22] It is known that ceria-based electrolytes may allow lower-temperature opera-

* To whom correspondence should be addressed. E-mail: balducci@univ.trieste.it.
† Universita' degli Studi di Trieste.
‡ University of Surrey.

(1) Taylor, K. C. In *Catalysis − Science and Technology*, Vol. 5; Anderson, J. R., Boudart, M., Eds.; Springer-Verlag: Berlin, 1984.
(2) Putna, E. S.; Bunluesin, T.; Fan, X. L.; Gorte, R. J.; Vohs, J. M.; Lakis, R. E.; Egami, T. *Catal. Today* **1999**, *50*, 343.
(3) Kašpar, J.; Fornasiero, P.; Graziani, M. *Catal. Today* **1999**, *50*, 285.
(4) Daturi, M.; Bion, N.; Saussey, J.; Lavalley, J. C.; Hedouin, C.; Seguelong, T.; Blanchard, G. *Phys. Chem. Chem. Phys.* **2001**, *3*, 252.
(5) Fornasiero, P.; Kašpar, J.; Graziani, M. *Appl. Catal. B* **1999**, *22*, L11.
(6) Balducci, G.; Kašpar, J.; Fornasiero, P.; Graziani, M.; Islam, M. S.; Gale, J. D. *J. Phys. Chem. B* **1997**, *101*, 1750.
(7) Balducci, G.; Kašpar, J.; Fornasiero, P.; Graziani, M.; Islam, M. S. *J. Phys. Chem. B* **1998**, *102*, 557.
(8) Balducci, G.; Islam, M. S.; Kašpar, J.; Fornasiero, P.; Graziani, M. *Chem. Mater.* **2000**, *12*, 677.
(9) Islam, M. S.; Balducci, G. In *Catalysis by Ceria and Related Materials*, Vol. 2; Trovarelli, A., Ed.; Imperial College Press: London, 2002.
(10) Machida, M.; Uto, M.; Kurogi, D.; Kijima, T. *J. Mater. Chem.* **2001**, *11*, 900.
(11) Nigge, U.; Wiemhofer, H. D.; Romer, E. W. J.; Bouwmeester, H. J. M.; Schulte, T. R. *Solid State Ionics* **2002**, *146*, 163.
(12) Deganello, F.; Martorana, A. *J. Solid State Chem.* **2002**, *163*, 527.
(13) Harrison, P. G.; Ball, I. K.; Azelee, W.; Daniell, W.; Goldfarb, D. *Chem. Mater.* **2000**, *12*, 3715−3725.
(14) McBride, J. R.; Hass, K. C.; Poindexter, B. D.; Weber, W. H. *J. Appl. Phys.* **1994**, *76*, 2435.
(15) Bernal, S.; Blanco, G.; Cifredo, G.; Perezomil, J. A.; Pintado, J. M.; Rodriguez-Izquierdo, J. M. *J. Alloys Compd.* **1997**, *250*, 449.
(16) Terribile, D.; Trovarelli, A.; Deleitenburg, C.; Primavera, A.; Dolcetti, G. *Catal. Today* **1999**, *47*, 133.
(17) Steele, B. C. H. *Solid State Ionics* **2000**, *129*, 95.
(18) Mogensen, M.; Sammes, N. M.; Tompsett, G. A. *Solid State Ionics* **2000**, *129*, 63.
(19) Wang, S.; Inaba, H.; Tagawa, H.; Hashimoto, T. *J. Electrochem. Soc.* **1997**, *144*, 4076.

10.1021/cm021289h CCC: $25.00
Published on Web 09/05/2003

tion of SOFCs, although there can be problems associated with electronic conductivity.[20]

The present paper is a contribution to the further understanding of the influence of aliovalent dopants upon the Ce^{4+}/Ce^{3+} reduction process in ceria. For this purpose, we have made use of computer simulation techniques to examine the energetics of Ce^{4+}/Ce^{3+} reduction in doped systems of the type $Ce_{(1-x)}M_xO_{2-x/(v-1)}$, where M is either divalent ($v = 2$; M = Mn, Ni, Zn, Ca) or trivalent ($v = 3$; M = Mn, Sc, Y, Gd, La). It should be noted that our investigation complements previous computational work on oxygen ion migration and dopant−vacancy association,[6,23−25] which is not the focus of this paper.

Computational Methods

The atomistic simulation of ionic materials is a well-established computational tool for which comprehensive accounts can be found in the literature.[26−28] For this reason, only a concise description will be given here.

The constituent ions of the solid are treated as classical charged particles interacting with each other through long-range (Coulombic) and short-range pair potentials. The short-range interactions are represented by suitable analytical functions of the interatomic separation; in this work, the Buckingham function was employed:

$$\Phi_{ij} = A_{ij}\exp\left(-\frac{r_{ij}}{\rho_{ij}}\right) - \frac{C_{ij}}{r_{ij}^6} \qquad (2)$$

in which the interaction energy Φ_{ij} involving ions i and j at distance r_{ij} depends on three empirical parameters A_{ij}, ρ_{ij}, and C_{ij}. The parameters describing the $Ce^{4+}\cdots O^{2-}$, $Ce^{3+}\cdots O^{2-}$, and $O^{2-}\cdots O^{2-}$ short-range interactions were those already used in our previous work,[6] in which the observed CeO_2 structure was correctly reproduced. The potential parameters for the dopants (M) were taken from the work of Lewis and Catlow[29] (Table 1). A potential cutoff of 15 Å was used in all cases.

Ionic polarizability was taken into account for the Ce^{3+}, Ce^{4+} and O^{2-} species through the shell model,[30] in which an ion is represented as a massive core connected to a massless shell by a harmonic spring. The formal ionic charge is suitably partitioned between the core and the shell, which can move relative to each other under the effect of the electric field generated by the surrounding crystal, thus simulating an induced dipole moment. The dopant ions were assumed to be unpolarizable: indeed, recent atomistic simulations of similar systems indicate that cationic polarizability has little influence on the results.[23] We have carried out similar preliminary calculations on our doped systems, which also indicate negligible influence on the overall results.

Table 1. Potential Parameters Used to Model the Solid Solutions

Short-Range Potential Parameters

$i - j$	A_{ij}(eV)	ρ_{ij}(Å)	C_{ij}(eV Å^6)	ref
O^{2-}-O^{2-}	22764.3	0.149	27.89	44
Ce^{4+}-O^{2-}	1986.83	0.35107	20.4	45
Ce^{3+}-O^{2-}	1731.6181	0.36372	14.433	45
Mn^{2+}-O^{2-}	832.7	0.33720	0.00	29
Ni^{2+}-O^{2-}	641.2	0.33720	0.00	29
Zn^{2+}-O^{2-}	700.3	0.33720	0.00	29
Ca^{2+}-O^{2-}	1227.7	0.3372	0.00	29
Mn^{3+}-O^{2-}	1257.9	0.3214	0.00	29
Sc^{3+}-O^{2-}	1299.4	0.3312	0.00	29
Y^{3+}-O^{2-}	1345.1	0.3491	0.00	29
Gd^{3+}-O^{2-}	1336.8	0.3551	0.00	29
La^{3+}-O^{2-}	1439.7	0.3651	0.00	29

Shell Model Parameters: $E_{\text{core-shell}}(r) = 1/2k_2r^2$

ion[a]	shell charge (e)	k_2(eV Å^{-2})	ref.
O^{2-}	−2.077	27.29	44
Ce^{4+}	7.7	291.75	45
Ce^{3+}	7.7	291.75	45

[a] All M dopants were treated as rigid ions.[29]

Defects were treated with a two-region methodology in which the crystal is partitioned into two spherical regions. The inner region 1 is centered on the defect and here the ions are relaxed individually under the defect perturbation. In the outer region 2, which extends theoretically to infinity, the larger distance from the defect allows the treatment of ionic relaxation by using approximate Mott−Littleton quasi-continuum procedures.[31] For this kind of treatment to work, it is crucial that proper convergence of the defect energies upon increasing the size of region 1 is achieved. In our case, this criterion was fulfilled when the number of ions contained in region 1 was greater than 750.

The different compositions of the systems investigated were simulated with a "mean field" approach, in which the solid solution $Ce_{(1-x)}M_xO_{2-x/(v-1)}$ is modeled as an AB_2 system of the same fluorite structure, with A and B being a "hybrid" cation and anion, respectively. The oxygen vacancies, which compensate for the lower charge of the aliovalent dopant in the real system, are modeled with a lower fractional occupancy of the anionic sites in the hybrid system. The properties of the hybrid species are averages of those of the pure species, according to the corresponding site occupancies. The interaction potential between any two crystallographic sites becomes scaled by the fractional occupancies. For example, the cation−anion short-range potential $\Phi_{A,B}$ is

$$\Phi_{A,B} = (1-x)\left(1-\frac{x}{2(v-1)}\right)\Phi_{\text{Ce,O}} + x\left(1-\frac{x}{2(v-1)}\right)\Phi_{\text{M,O}}$$

The above computational methodologies are implemented in the GULP code,[32] which was used throughout this work.

(20) Tuller, H. L.; Nowick, A. S. *J. Chem. Phys. Solids* **1977**, *38*, 859.
(21) Murray, E. P.; Tsai, T.; Barnett, S. A. *Nature* **1999**, *400*, 649.
(22) Kharton, V. V.; Figueiredo, F. M.; Navarro, L.; Naumovich, E. N.; Kovalevsky, A. V.; Yaremchenko, A. A.; Viskup, A. P.; Carneiro, A.; Marques, F. M. B.; Frade, J. R. *J. Mater. Sci.* **2001**, *36*, 1105.
(23) Minervini, L.; Zacate, M. O.; Grimes, R. W. *Solid State Ionics* **1999**, *116*, 339.
(24) Catlow, C. R. A. *Solid State Ionics* **1984**, *12*, 67.
(25) Kilner, J. A. *Solid State Ionics* **1983**, *8*, 201.
(26) Catlow, R. C. A., Ed.; *Computer Modelling in Inorganic Crystallography*; Academic Press: London, 1997.
(27) Catlow, C. R. A., Mackrodt, W. C., Eds.; *Computer Simulation of Solids*; Springer: Berlin, 1982.
(28) Catlow, C. R. A.; Ackermann, L.; Bell, R. G.; Cora, F.; Gay, D. H.; Nygren, M. A.; Pereira, J. C.; Sastre, G.; Slater, B.; Sinclair, P. E. *Faraday Discuss.* **1997**, *106*, 1.
(29) Lewis, G. V.; Catlow, C. R. A. *J. Phys. C: Solid State Phys.* **1985**, *18*, 1149.
(30) Dick, B. G.; Overhauser, A. W. *Phys. Rev.* **1958**, *112*, 90.
(31) Mott, N. F.; Littleton, M. J. *Trans. Faraday Soc.* **1938**, *34*, 485.

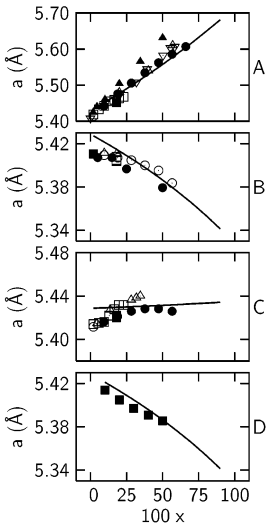

Figure 1. Comparison of calculated lattice parameter (a) as a function of composition (x in $Ce_{(1-x)}M_xO_{(2-x/(v-1))}$) with available experimental data. Graph A refers to the $Ce_{(1-x)}La_xO_{(2-x/2)}$ system: the solid line shows calculated values; symbols indicate experimental values taken from the following sources: □[46] ■[47] ○[48] ●[49] △[15] ▲[14] ▽.[34] Graph B refers to the $Ce_{(1-x)}Y_xO_{(2-x/2)}$) system: the solid line shows calculated values; symbols indicate experimental values taken from the following sources: □[47] ■[48] ○[49] ●[50] △.[51] Graph C refers to the $Ce_{(1-x)}Gd_xO_{(2-x/2)}$ system: the solid line shows calculated values; symbols indicate experimental values taken from the following sources: □[46] ■[47] ○[48] ●[49] △.[14] Graph D refers to the $Ce_{(1-x)}Sc_xO_{(2-x/2)}$ system: the solid line shows calculated values; symbols indicate experimental values taken from reference 23.

Results and Discussion

Structural Modeling. Because many dopants are able to dissolve into ceria to give true solid solutions retaining the fluorite structure up to quite large x values,[10,14,15,33−36] we have performed simulations for $0.1 \le x \le 0.5$. We are aware, however, that the highest x values may not be attained by some of the dopant species considered in this work.

The reliability of the potential parameters used for the simulations was assessed by comparing the calculated lattice constants of the solid solutions as a function of composition with the available experimental values. The results are summarized in Figures 1 and 2.

The figures reveal a satisfactory agreement over a wide range of compositions for the La, Y, Gd, and Sc dopants, for which several sources of experimental data are available in the literature. This agreement is despite the significant scatter of some of the experimental lattice parameter data, which probably reflects variations in the distribution of the dopant ions caused by different thermal conditions during the synthesis procedure.[17] Moreover, for all the dopants considered, the calculated lattice constant varies with dopant content in close accord with the empirical formula of Kim,[37]

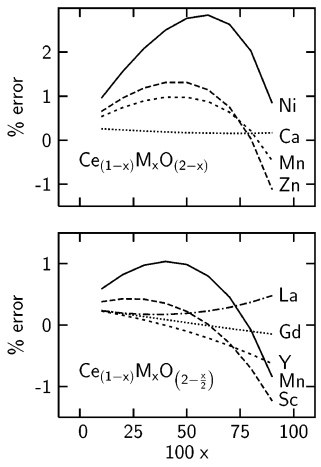

Figure 2. Percent error of the calculated lattice parameter with respect to the value predicted by Kim's empirical formula[37] as a function of the composition for the divalent (upper) and trivalent (lower) dopants.

which, for the present case of $Ce_{(1-x)}M_xO_{2-x/(v-1)}$ solid solutions, reads

$$d = 0.5413 + (0.022\Delta r + 0.00015\Delta z)100x \quad (3)$$

where d is the lattice parameter of the solid solution in nanometers, Δr is the difference between the ionic radius of the dopant and that of Ce^{4+}, and $\Delta z = v - 4$.

Figure 2 shows the percentage error of the calculated lattice parameter with respect to Kim's prediction as a function of composition. The relative error is within 1% in all cases, except for Ni, where 3% is reached. We attribute this to the uncertainty in the ionic radius of Ni^{2+}, which was estimated for coordination number 8 from the corresponding value for coordination number 6 from Shannon,[38] with a procedure similar to that used by Minervini et al.[23] Finally, we note that the experimental value of 5.3954 Å reported for the lattice constant of the $Ce_{0.9}Zn_{0.1}O_{1.9}$ system[39] compares well with our calculated value of 5.4027 Å.

Ce^{4+}/Ce^{3+} Reduction. The ability of cerium to switch between the +4 and +3 oxidation states is a key feature of ceria. This redox process in ceria-based oxides is crucial not only for its oxygen buffering capabilities, but also for its catalytic activity in a number of reactions.[10,16,40,41] In addition, it has been known for many years that the reduction process in ceria-based electrolytes to form Ce^{3+} localized electronic defects introduces electronic conduction (involving a small polaron hopping mechanism).[20] When the reductant is the lattice oxygen (eq. 1), the detailed description of the Ce^{4+}/Ce^{3+} reduction process is as follows:

$$2Ce_{Ce}^{\times} + O_O^{\times} = 2Ce'_{Ce} + V_O^{\bullet\bullet} + \frac{1}{2}O_{2(g)} \quad (4)$$

where we use Kröger−Vink notation for the Ce^{3+} (Ce'_{Ce}) and oxygen vacancy ($V_O^{\bullet\bullet}$) defects. When ceria is

(32) Gale, J. D. *J. Chem. Soc., Faraday Trans.* **1997**, *93*, 629.
(33) Lamonier, C.; Ponchel, A.; D'Huysser, A.; Jalowiecki-Duhamel, L. *Catal. Today* **1999**, *50*, 247.
(34) Morris, B. C.; Flavell, W. R.; Mackrodt, W. C.; Morris, M. A. *J. Mater. Chem.* **1993**, *3*, 1007.
(35) Kudo, T.; Obayashi, H. *J. Electrochem. Soc.* **1975**, *122*, 142.
(36) Chen, H.; Sayari, A.; Adnot, A.; Larachi, F. *Appl. Catal. B* **2001**, 195.
(37) Kim, D. J. *J. Am. Ceram. Soc.* **1989**, *72*, 1415.
(38) Shannon, R. D. *Acta Crystallogr.* **1976**, *A32*, 751.
(39) Zhang, Y.; Andersson, S.; Muhammed, M. *Appl. Catal. B* **1995**, *6*, 325.
(40) de Carolis, S.; Pascual, J. L.; Pettersson, L. G. M.; Baudin, M.; Wojcik, M.; Hermansson, K.; Palmqvist, A. E. C.; Muhammed, M. *J. Phys. Chem. B* **1999**, *103*, 7627.
(41) Palmqvist, A. E. C.; Johansson, E. M.; Jaras, S. G.; Muhammed, M. *Catal. Lett.* **1998**, *56*, 69.

Table 2. Calculated Reduction Energy (eV) for Divalent and Trivalent Dopants in Bulk Ceria at 10% and 50% Levels[a]

	ionic radius (Å)	10%	50%
	Divalent Dopants		
Ni	0.813	6.99	4.42
Zn	0.90	6.98	4.34
Mn	0.96	6.98	4.20
Ca	1.12	6.94	3.85
	Trivalent Dopants		
Mn	0.766	7.38	7.00
Sc	0.87	7.31	6.58
Y	1.019	7.27	6.02
Gd	1.053	7.22	5.75
La	1.16	7.08	5.15

[a] For each dopant, the ionic radius (in Å) has been reported.[38] The ionic radii of Ni^{2+} and Mn^{3+} for coordination number 8 was estimated with a procedure similar to that reported in reference 23. The detailed procedure for the calculation of the Ce^{4+}/Ce^{3+} reduction energy is outlined in ref. 8. The needed ionization and dissociation energy contributions are as follows. Fourth ionization potential of cerium, 36.26 eV; first and second electron affinity of oxygen, 7.29 eV; bond dissociation energy of dioxygen, 2.58 eV per oxygen atom.

doped with a di- or trivalent cation, a mean field description of the resulting solid solution is adopted. The reduction energy can then be evaluated across the composition range by combining the formation energies of the component defects (Ce'_{Ce} and $V_O^{\bullet\bullet}$) and taking into account the hybrid species in the mixed oxide. The procedure has been detailed in ref 8, and the appropriate dissociation and ionization energy contributions are reported in Table 2. The merit of our simulation approach is that it includes detailed estimates of lattice polarization (relaxation) and Coulomb energies, which are difficult to make from other sources.

The present study complements previous simulation work on oxygen migration and dopant−vacancy association in these doped systems.[6,23−25] This early work showed that the binding energy for dopant vacancy clusters correlates with ion size with the lowest energy for Gd^{3+} (leading to optimum oxygen ion conductivity). It should be stressed that we consider solid solutions of the type $Ce_{(1-x)}M_xO_{2-x/(v-1)}$ with a homogeneous distribution of dopant ions and oxygen vacancies, rather than isolated defect clusters, in which defect interactions are implicitly included in the calculations.

The results of our calculations of reduction energies as a function of divalent and trivalent dopant content are shown in Figure 3 (and listed in Table 2 for the lowest and highest dopant levels).

Two main points emerge. First, we note that in each case the Ce^{4+}/Ce^{3+} reduction energy decreases significantly with increasing dopant content, with the decrease being more pronounced for the divalent dopants. The magnitude of the values are very similar for the divalent dopants. Although it is difficult to make direct comparisons with measurements, our calculated energies are consistent with values of 4.7−5.0 eV for the relative partial molar enthalpy per oxygen atom in bulk ceria.[19,42] We should also note that the calculated reduction energies are likely to be lower at the surfaces of the doped systems, as found in previous simulation work

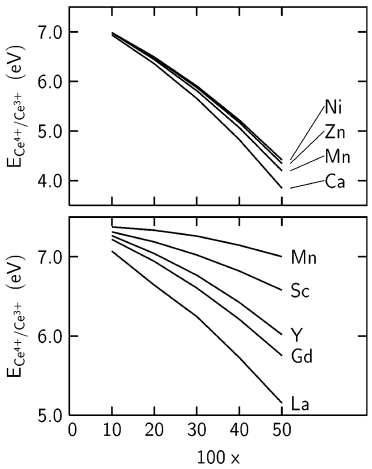

Figure 3. Ce^{4+}/Ce^{3+} reduction energy as a function of composition (x in $Ce_{(1-x)}M_xO_{2-x/(v-1)}$) for the series of divalent ($v = 2$, upper) and trivalent ($v = 3$, lower) dopants.

on the (110), (111), and (310) surfaces of pure ceria and CeO_2-ZrO_2 solid solutions.[7] This is a topic for future investigation.

Second, there is a trend with ionic size: for the same dopant concentration, larger dopants are more effective in promoting the Ce^{4+}/Ce^{3+} reduction. These results may be rationalized in terms of the increase in ionic size associated with the Ce^{4+}/Ce^{3+} reduction ($r_{Ce^{4+}} = 0.97$ Å, $r_{Ce^{3+}} = 1.143$ Å[38]). The oxygen vacancies generated by acceptor doping may assist in accommodating the greater relaxation or elastic strain associated with forming the larger Ce^{3+} species. This explains the overall decrease of the reduction energy with increasing dopant concentration. The lower reduction energies obtained for the divalent ions as compared with the trivalent ions for the same dopant level are the result of divalent dopants inducing twice the number of oxygen vacancies, as can be seen by plotting the reduction energy as a function of the oxygen vacancy concentration. Moreover, for a fixed dopant or oxygen vacancy concentration, an increase in the ionic size of the dopant produces a lattice expansion which is also effective in relieving the stress caused by the Ce^{4+}/Ce^{3+} reduction. This is reflected also by the average relaxation of the nearest-neighbor oxygen ions away from the Ce^{3+} center as a function of the dopant size: for instance, it amounts to about 0.1 Å for 50% CaO doped ceria, but increases to about 0.15 Å for NiO doped ceria at the same dopant level.

We note that there is some evidence that if the dopant oxide exhibits redox properties both the kinetics and the extent of CeO_2 reduction are strongly influenced, which warrants further investigation.

The promotion of cerium reducibility by acceptor dopants has been reported in several experimental studies.[16,33,39,40] For example, Steele[17,43] found that for

(42) Chang, E. K.; Blumenthal, R. N. *J. Solid State Chem.* **1988**, *72*, 330.
(43) Steele, B. C. H.; Hori, K. M.; Uchino, S. *Solid State Ionics* **2000**, *135*, 445.
(44) Dwivedi, A.; Cormack, A. N. *Philos. Magn. A* **1990**, *61*, 1.
(45) Sayle, T. X. T.; Parker, S. C.; Catlow, C. R. A. *Surf. Sci.* **1994**, *316*, 329.
(46) Hong, S. J.; Virkar, A. V. *J. Am. Ceram. Soc.* **1995**, *78*, 433.
(47) Etsell, T. H.; Flengas, S. N. *Chem. Rev.* **1970**, *70*, 339.
(48) Gerhardt-Anderson, R.; Nowick, A. S. *Solid State Ionics* **1981**, *5*, 547.
(49) Inaba, H.; Tagawa, H. *Solid State Ionics* **1996**, *83*, 1.

CeO_2−rare-earth solid solutions it becomes easier to reduce Ce^{4+} to Ce^{3+} as the rare-earth concentration increases (at a given oxygen partial pressure and temperature). Our calculations support these observations, thereby providing relative trends based on quantitative calculations as opposed to qualitative arguments.

In a recent paper, de Carolis et al. studied the (110) surface of the $Ce_{0.875}Ca_{0.125}O_{1.875}$ solid solution with molecular dynamics (MD) and ab initio simulation techniques.[40] Their calculations indicate that the transfer of one electron from a neighboring oxide ion to a Ce^{4+} cation is significantly favored by doping, as a result of the reduced coordination number of the cerium ion due to the presence of oxygen vacancies. Our results generalize these findings for a whole series of dopants and indicate that the creation of oxygen vacancies in the fluorite structure of doped cerias is effective in promoting the reducibility of cerium not only dynamically, but also at a purely energetic level.

Concluding Remarks

Computer simulation techniques have been used to investigate the energetics of the Ce^{4+}/Ce^{3+} reduction process in CeO_2−MO (M = Ca, Mn, Ni, Zn) and CeO_2−M_2O_3 (M = Sc, Mn, Y, Gd, La) solid solutions. Our atomistic approach has generated quantitative estimates of the relative reduction energies, which provide a useful systematic examination of the reducibility for different dopant species. (1) Calculated structural lattice parameters are in satisfactory accord with the available experimental determinations over a wide range of compositions. (2) The Ce^{4+}/Ce^{3+} reduction process is enhanced with increasing dopant content, in accord with observation. The enhancement is more pronounced for divalent dopants; i.e., for significant dopant levels, it is easier to reduce divalent-doped than trivalent-doped (or undoped) ceria. (3) For a fixed dopant level or oxygen vacancy concentration, the reduction of cerium is more favorable for larger dopant ions (e.g., Ca^{2+}, La^{3+}). This result may be explained in terms of the larger dopant size being effective in accommodating the greater relaxation or elastic strain associated with forming the larger Ce^{3+} species upon reduction.

These calculated trends in reduction energetics are of relevance to oxygen storage in automotive three-way catalysts and to fuel cell applications. Because reduction is less favorable for trivalent ions on energetic grounds, our results also suggest that trivalent-doped ceria (e.g., Sc, Gd) is preferred over divalent-doping for use as SOFC electrolytes to minimize Ce^{3+} formation and contributions from electronic conductivity.

Acknowledgment. G.B. is grateful to Prof. R. Grimes for kindly providing unpublished work. G.B. acknowledges financial support for a scientific visit from the Italian CNR, under the “Short-Term Mobility Anno 2001” program.

CM021289H

(50) Hartridge, A.; Krishna, M. G.; Bhattacharya, A. K. *Int. J. Mod. Phys. B* **1998**, *12*, 1573.

(51) Li, P.; Chen, I. W.; Penner-Hahn, J. E.; Tien, T. Y. *J. Am. Ceram. Soc.* **1991**, *74*, 958.